Available online at www.sciencedirect.com
ScienceDirect
Polymer 47 (2006) 6464–6471
polymer
www.elsevier.com/locate/polymer

An explanation of increased hydrolysis of the β-(1,4)-glycosidic linkages of grafted cellulose using molecular modeling

David T. Karst [a], Yiqi Yang [a,b,*], Genzo Tanaka [c]

[a] Department of Textiles, Clothing and Design, 234 HE Building, University of Nebraska – Lincoln, Lincoln, NE 68583-0802, United States
[b] Department of Biological Systems Engineering, 234 HE Building, University of Nebraska – Lincoln, Lincoln, NE 68583-0802, United States
[c] Network Computing Services, Inc. and Army High Performance Research Center, 1200 Washington Avenue, S., Minneapolis, MN 55415, United States

Received 15 May 2006; received in revised form 2 July 2006; accepted 3 July 2006
Available online 24 July 2006

Abstract

Grafting various groups onto cellulose is found to substantially increase acid hydrolysis of the β-(1,4)-glycosidic linkages. Molecular modeling is used to explain how various substituents such as esters and ethers cause this phenomenon. A substituent helps stabilize hydrolyzed cellulose by serving as an anchor to the end of the cleaved cellulose to which it is bonded, making it less mobile, and allowing it to have stronger interactions than those in pure hydrolyzed cellulose. Hydrolysis increases with increasing size of the substituent. Molecules sorbed but not grafted to cellulose do not increase hydrolysis. Hydrolysis mainly occurs at glucoses bonded to the substituent, and supporting experiments show that hydrolysis approaches equilibrium when no substituent remains on the cellulose fiber.

Keywords: Hydrolysis; Cellulose; Molecular modeling

1. Introduction

Cellulose is one of the most abundant polymers in the world, and hydrolysis of the β-(1,4)-glycosidic linkages is an important reaction. It leads to dramatic strength loss of cellulosic material, and therefore resistance to hydrolysis is important for cellulosic materials requiring good strength such as construction materials and packaging. The resistance of cellulose to hydrolysis is also important for textiles, composites, and paper since there is great interest in using cellulose fibers from agricultural byproducts for these materials [1–4]. On the other hand, hydrolysis of the glycosidic linkages is important for the conversion of cellulose to glucose that is used in fermentation to produce ethanol and other alcohols, acids, ketones, and many other ''green'' chemicals. However, the percent conversion of cellulose to glucose is very low [5].

Acid and thermal energy increase hydrolysis of the glycosidic linkage. Substitution of the hydroxyl groups on cellulose also has resulted in greater hydrolysis compared to non-substituted cellulose [6–9]. It is therefore important to consider hydrolysis in applications that involve grafting groups onto cellulose such as the production of cellulose acetate, carboxymethyl cellulose, and other cellulose derivatives. Grafting of the reactive dyes C.I. Reactive Blue 19 (Blue 19), C.I. Reactive Black 5, or C.I. Reactive Red 120 onto cellulose in cotton fabric have been found to increase acid hydrolysis of cellulose after it undergoes a commercial laundering process, which includes alkaline suds steps with each followed by a rinse, a weak acidic bath at pH 4.0–4.5, and a pressing step at 154 °C. Approaching hydrolysis equilibrium, the DP of the cellulose bonded to Blue 19 was only 31% of the non-substituted cellulose DP. Cellulose with C.I. Direct Red 80 sorbed onto the fiber without substitution has not shown greater hydrolysis than non-substituted cellulose [9]. Cellulose

* Corresponding author. Department of Textiles, Clothing and Design, 234 HE Bldg, University of Nebraska – Lincoln, Lincoln, NE 68583-0802, United States. Tel.: +1 402 472 5197; fax: +1 402 472 0640.
E-mail address: yyang2@unl.edu (Y. Yang).

0032-3861/$ - see front matter © 2006 Elsevier Ltd. All rights reserved.
doi:10.1016/j.polymer.2006.07.006

sulfite and cellulose sulfate in wood pulp have been observed to have rates of hydrolysis that are twice that of non-substituted cellulose in cotton linters [8]. Increased hydrolysis at pH 1.2 and 80 °C has been seen in cellulose with the aldehyde group grafted onto cellulose. After accelerated aging, the DP of the aldehydocellulose was only 5.5% of the non-substituted cellulose DP [7]. The rate constant for hydrolysis of carboxymethyl cellulose in 2.5 M HCl at 60 °C has been found to increase from 1 to 9 min^{-1} along with an increase in the extent of hydrolysis as the degree of substitution increases. Approaching hydrolysis equilibrium, the DP of the carboxymethyl cellulose with the greatest degree of substitution was only 45% of the non-substituted cellulose DP [6].

It is thought that a substituent on the glucose residual on the reducing end side increases acid hydrolysis of the glycosidic linkage by inducing the transfer of electrons from the first carbon in the glucose residual on the non-reducing end side to the oxygen in the glycosidic linkage [6,8,9]. This theory comes from the fact that in the second step of acid hydrolysis of cellulose, an electron is transferred from the first carbon in the glucose residual on the non-reducing end side to the oxygen in the glycosidic linkage [10]. However, this inductive effect decreases with increasing distance from the electron withdrawing group and charged center, and in the case of cellulose, the substituent is three to four sigma bonds away from the nearest glycosidic linkage.

Given the limited literature explaining why a substituent on cellulose increases acid hydrolysis of the glycosidic linkage, this phenomenon is not fully understood. To further our understanding, one objective of this current study was to explain why a substituent increases acid hydrolysis of the β-(1,4)-glycosidic linkage. Another goal was to find if this phenomenon can be studied using molecular modeling because to the best of our knowledge, it has not been used to study this topic.

2. Experimental

2.1. Molecular modeling simulations

The molecular modeling software used for this study was MS Modeling 3.0, available from Accelrys [11]. The methodology used in our earlier study for the hydrolysis of PLA was used to model the hydrolysis of the glycosidic linkages of cellulose [12]. Using the Amorphous Cell module of MS Modeling 3.0, an amorphous unit cell was generated that modeled a unit volume of amorphous cellulose. Because of computing limitations, the amorphous unit cell was created as five cellulose molecules with 20 cellobiose units per molecule at a density of 1.31 g/cm^3. This amorphous density of cellulose was based on an overall cellulose fiber density of 1.50 g/cm^3, a crystalline density of 1.58 g/cm^3, and a crystallinity of 70% [13–15].

The effect of a substituent on hydrolysis of the β-(1,4)-glycosidic linkage of cellulose was studied for various substituents such as the carboxymethyl (OCH_2COOH), mono-substituted acetyl ($OCOCH_3$), and tri-substituted acetyl groups. C.I. Reactive Blue 19 (Blue 19), which has an anthraquinone parent structure and bonds to cellulose by an ether linkage, was another substituent selected for this study since experimental data are available for hydrolysis of cellulose bonded to this molecule. Other substituents included various quaternary ammonium compounds based on $OCH_2CHOHCH_2N(CH_3)_2X$, which we refer to as X quat where X is CH_3, CH_2OH, $C_{18}H_{37}$, $CH_2(OCH_2CH_2)_6OH$, or C_6H_5. One substituent molecule was grafted to one cellulose molecule in the structure by an ether linkage at the sixth carbon position of the number 20 glucose residual, which is a non-reducing end side glucose. To model the effect of a non-bonded molecule, C.I. Reactive Blue 19 was placed in the cellulose structure at the same position as the grafted Blue 19 but without a covalent bond with cellulose.

For hydrolysis of each structure, we cleaved the glycosidic linkage between the number 20 and 21 glucose residual of the cellulose molecule containing the substituent to form two cleaved segments of identical DP. These two segments were separated by translation and rotation of the non-reducing end segment such that the distance between their end hydroxyl groups was greater than 10 Å because this was the non-bonded cut-off. The non-bonded cut-off is the distance between any two atoms beyond which their van der Waals interactions are neglected. The non-bonded cut-off was set at 10 Å since this is within half of the unit cell length of 34.51 Å. This cut-off is conventionally used in molecular modeling of macromolecules [16,17]. To calculate the total electrostatic interactions, the cell multipole method was used, which calculates the electrostatic interactions between groups of atoms that are grouped based on their location in the unit cell. With this method, each atom was regrouped when its position in the cell moved by more than 1 Å.

To minimize the energy of the cellulose structures, molecular dynamics simulations and energy minimizations were run using the Amorphous Cell and Discover modules of MS Modeling 3.0. The polymer consistent force field (PCFF) was the set of parameters used by these modules to calculate the potential energy of the cellulose structures. The PCFF was chosen since it is accurate for modeling polymers, and partial charges were assigned to each atom according to this force field [18–20]. During each run, the ''check for ring catenations'' option was used in Amorphous Cell so that a bond or a glucose ring would not penetrate the interior of another glucose ring. Beginning with each unhydrolyzed cellulose structure, an energy minimization was first performed using the conjugate gradient method with convergence criteria of 0.1 kcal/mol per Å. A molecular dynamics (MD) simulation was then performed on this structure using a constant volume/constant temperature ensemble at 373 K. This temperature was selected because hydrolysis of Blue 19-substituted cellulose and pure cellulose has been observed after commercial laundering, and Yang and Hughes have stated that the hydrolysis mainly occurred during the pressing step in which the temperature of the cellulose was 373 K [9]. The MD simulation was performed for 500,000 steps with a time step of 10^{-15} s and with an equilibration time of 500×10^{-12} s. The final snapshot of the MD simulation was selected for the next energy minimization because

at this point in the MD simulation, the potential energy oscillated within ±125 kcal/mol. An energy minimization was then performed on this structure using the conjugate gradient method and convergence criteria of 0.1 kcal/mol per Å. After the energy minimization of each unhydrolyzed cellulose structure, the cellulose was cleaved as described above to create the hydrolyzed cellulose structures. After separating the cleaved segments, an energy minimization, MD simulation, and another energy minimization were performed using the same simulation conditions specified for the unhydrolyzed celluloses. For each condition, MD simulations/energy minimizations were performed five times for the unhydrolyzed and hydrolyzed structures of the substituted cellulose and pure cellulose. This many simulations were required to ensure that the conformations of the cellulose structures were energy minimized to the extent that the differences between the energies of the hydrolyzed and unhydrolyzed structures did not change by more than 5% after repeated simulations.

Mechanical agitation of the cellulose fiber was not considered in the molecular modeling because when mechanical agitation results in breakage of fiber, it is mainly due to the polymer chains slipping past each other without breakage of covalent bonds [21].

2.2. Analysis of molecular modeling data

The change in potential energy for hydrolysis was used to evaluate how readily the substituted cellulose and pure cellulose undergo hydrolysis. The change in potential energy for hydrolysis was calculated according to Eq. (1).

$$\Delta U = U_{\text{hyd}} - U_{\text{unhyd}} - U_{\text{w}} \tag{1}$$

In Eq. (1), ΔU is the change in potential energy for the acid hydrolysis of cellulose. U_{unhyd} is the potential energy of the cellulose structure before hydrolysis, U_{hyd} is its potential energy after hydrolysis, and U_{w} is the potential energy of one water molecule isolated from the system. The potential energy values were obtained from the molecular modeling simulations.

To explain the effect of the size of the substituent on the ΔU, the total volume that each substituent occupies in the energy minimized cellulose structures was obtained after hydrolysis. This total volume is defined as the van der Waals volume of the substituent plus the surrounding empty volume that cannot be occupied by other molecules in the energy minimized system. To calculate the volume of a substituent, we took the substituent from the hydrolyzed cellulose structure and broke up the substituent into parts such that each part can fit inside a separate rectangular box, which is the smallest box that can contain all the atoms of that part of the substituent. The volumes of the boxes were summed to obtain the volume of the substituent. A rectangular box was the geometry used to measure the volume since it was the only geometry available with the molecular modeling software.

To evaluate how the interactions between each substituent and cellulose affect the hydrolysis of cellulose, their interaction energy was calculated according to Eq. (2).

$$U_{\text{substituent-cellulose}} = U_{\text{system}} - U_{\text{system/substituent}} - U_{\text{system/cellulose}} \tag{2}$$

In Eq. (2), $U_{\text{substituent-cellulose}}$ is the potential energy of the interaction between the substituent and the five cellulose molecules in the system. U_{system} is the potential energy of the entire system. $U_{\text{system/substituent}}$ is the potential energy of the system with the substituent deleted. $U_{\text{system/cellulose}}$ is the energy of the system with the five celluloses deleted.

To evaluate how the interactions between the cellulose molecules are affected by each substituent, the energy of the cellulose–cellulose interaction was calculated according to Eq. (3).

$$U_{\text{cellulose-cellulose}} = U_{\text{system/substituent}} - U_{\Sigma\text{celluloses}} \tag{3}$$

In Eq. (3), $U_{\text{cellulose-cellulose}}$ is the potential energy of the interactions between the five cellulose molecules. $U_{\Sigma\text{celluloses}}$ is the sum of the potential energies of each cellulose molecule isolated from the system.

To evaluate the mobility of the glucose residuals bonded to the substituent after cleavage, the mean square displacement (MSD) of those glucose residuals was obtained by running MD simulations for $100{,}000 \times 10^{-12}$ s at 100 °C.

2.3. Validation of molecular modeling

Since experimental data for the hydrolysis of pure cellulose and cellulose bonded to C.I. Reactive Blue 19 were available, these data were used to evaluate if the molecular modeling results were reasonable [9,22]. The DP of the Blue 19-substituted cellulose and pure cellulose were experimentally obtained after a certain number of commercial laundering cycles for the cellulosic fabric as listed in Table 1. Since data at the hydrolysis reaction equilibrium were not available, Eq. (4) was used to obtain the DP as hydrolysis approaches equilibrium. This empirical equation was chosen since it has been found to fit data for acid hydrolysis of cellulose consisting of crystalline and amorphous regions [23]. The Blue 19-substituted cellulose data had an R^2 of 0.993, and the pure cellulose data had an R^2 of 0.999.

Table 1
DP of non-substituted cellulose and Blue 19-substituted cellulose after certain numbers of commercial laundering cycles [22]

Commercial laundering cycles	K/S	Non-substituted cellulose DP	Blue 19-substituted cellulose DP
0	6.48	1876	1799
5	5.71	1662	1562
20	4.45	1452	1094
50	2.47	1311	951

Blue 19 is C.I. Reactive Blue 19.

Table 2
Calculated potential energies before (U_{unhyd}) and after hydrolysis (U_{hyd}), the change in potential energy for hydrolysis (ΔU) for the van der Waals forces (ΔU_{vdW}), for the electrostatic forces ($\Delta U_{electrostatic}$), and for the cellulose–cellulose interactions ($\Delta U_{cellulose-cellulose}$), and the potential energy of the substituent–cellulose interactions before ($U_{substituent-cellulose,\ unhyd}$) and after hydrolysis ($U_{substituent-cellulose,\ hyd}$)

Substituent	U_{unhyd}, kcal/mol	U_{hyd}, kcal/mol	ΔU, kcal/mol	ΔU_{vdW}, kcal/mol
$C_{18}H_{37}$ Quat	400	290	−110	−35
$CH_2(OCH_2CH_2)_6OH$ Quat	449	344	−105	−28
Blue 19	416	340	−76	−21
C_6H_5 Quat	473	413	−60	−18
CH_2OH Quat	412	358	−54	−13
CH_3 Quat	459	408	−51	−11
Tri-substituted acetyl	409	364	−45	−9
Carboxymethyl	443	406	−37	−8
Mono-substituted acetyl	471	441	−30	−1
N-B Blue 19	425	449	24	25
None	495	520	25	29

Substituent	$\Delta U_{electrostatic}$, kcal/mol	$\Delta U_{cellulose-cellulose}$, kcal/mol	$U_{substituent-cellulose,\ unhyd}$, kcal/mol	$U_{substituent-cellulose,\ hyd}$, kcal/mol
$C_{18}H_{37}$ Quat	−7	−241	−125	−126
$CH_2(OCH_2CH_2)_6OH$ Quat	−5	−235	−120	−121
Blue 19	−1	−198	−111	−110
C_6H_5 Quat	−5	−188	−90	−91
CH_2OH Quat	−4	−187	−83	−84
CH_3 Quat	−5	−181	−78	−77
Tri-substituted acetyl	−6	−170	−56	−55
Carboxymethyl	−5	−158	−48	−49
Mono-substituted acetyl	−9	−154	−34	−33
N-B Blue 19	−4	−103	−90	−91
None	−3	−107	N/A	N/A

Each value is for cellulose bonded to various substituents, cellulose with non-bonded C.I. Reactive Blue 19 (N-B Blue 19), and pure cellulose (None). X Quat is $OCH_2CHOHCH_2N(CH_3)_2X$, where X is $C_{18}H_{37}$, $CH_2(OCH_2CH_2)_6OH$, C_6H_5, CH_2OH, or CH_3. Blue 19 is C.I. Reactive Blue 19. All substituents are on the sixth carbon position on the reducing end side.

$$(DP - DP_0)^{-1} = (kt)^{-1} + (DP_{eq} - DP_0)^{-1} \quad (4)$$

In Eq. (4), k^{-1} is the slope of the best fit of a plot of $(DP - DP_0)^{-1}$ versus t^{-1}, and $(DP_{eq} - DP_0)^{-1}$ is the intercept. The t is the time, or number of launderings in this case, DP is the DP at time t, DP_0 is the DP at $t = 0$, and DP_{eq} is the DP when hydrolysis reaches equilibrium.

Values for the Kubelka–Munk function (K/S) were experimentally obtained for Blue 19-substituted cellulose after a certain number of commercial launderings as listed in Table 1 [22]. The K/S is directly proportional to the concentration of dye in a fiber [24]. The K/S of undyed bleached cotton 400 fabric is only 0.0816. Eq. (5) was therefore used to relate the K/S to the concentration of Blue 19.

$$K/S = A[\text{Blue 19}] + 0.0816 \quad (5)$$

In Eq. (5), [Blue 19] is the concentration of Blue 19 in the cellulose fiber, and A is the slope of a plot of K/S versus [Blue 19].

3. Results and discussion

3.1. ΔU for hydrolysis of pure and substituted cellulose

Molecular modeling was used to study the effect of a substituent on hydrolysis of the β-(1,4)-glycosidic linkage of cellulose. In Table 2, a more negative change in potential energy for hydrolysis (ΔU) indicates a greater tendency for hydrolysis, and the ΔU values for substituted cellulose are negative (−110 to −30 kcal/mol) while that of pure cellulose is positive (25 kcal/mol). The substantial difference in the ΔU values between substituted cellulose and pure cellulose indicates that all the substituents included in this study greatly increase hydrolysis of the glycosidic linkage.

As the volume of the substituent increases as shown in Fig. 1 from that of mono-substituted acetyl to that of

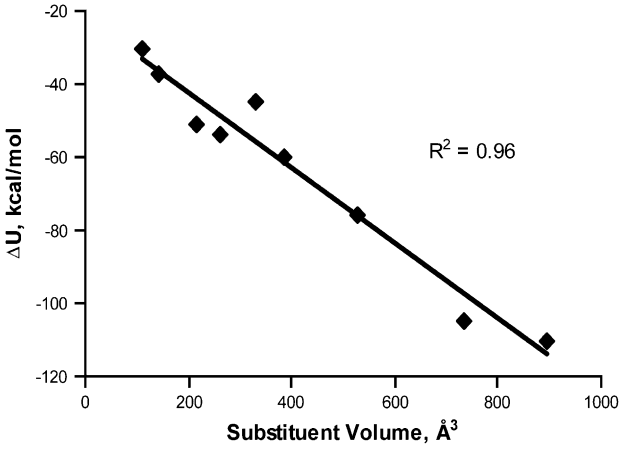

Fig. 1. Change in potential energy for hydrolysis of substituted cellulose (ΔU) versus the volume of the substituent.

$OCH_2CHOHCH_2N(CH_3)_2C_{18}H_{37}$ ($C_{18}H_{37}$ Quat), the ΔU becomes more negative, and a regression of ΔU versus substituent volume gives an R^2 of 0.96. There is therefore a strong relationship between the size of the substituent on cellulose and its ability to increase hydrolysis of the glycosidic linkages.

The statistical significance of the ΔU values is demonstrated by the high R^2 for the regression of the ΔU values versus the substituent volume. In addition, the molecular dynamics simulations and energy minimizations for the calculation of the U_{unhyd} and U_{hyd} values for the non-substituted cellulose and Blue 19-substituted cellulose were replicated. The U_{unhyd} and U_{hyd} values for Blue 19-substituted cellulose were 415 and 339 kcal/mol, respectively, and those for the non-substituted cellulose were 494 and 518 kcal/mol, respectively, which is a difference between replications within 0.40%. The ΔU values for these replications are −76 kcal/mol for Blue 19-substituted cellulose and 24 kcal/mol for non-substituted cellulose, which gives a difference in ΔU between replications within 4%.

3.2. Cause of increased hydrolysis

Substituted cellulose is more susceptible to acid hydrolysis of the glycosidic linkages because the substituent helps stabilize cellulose after hydrolysis as indicated in Table 2 by the 15–44% lower potential energy (U_{hyd}) of substituted cellulose relative to that of pure cellulose after hydrolysis. In addition, the change in potential energy of the cellulose–cellulose interactions in the system ($\Delta U_{cellulose-cellulose}$) is 44–125% more negative for the substituted celluloses than for the pure cellulose as indicated in Table 2. The substituents therefore allow for stronger cellulose–cellulose interactions after hydrolysis than are possible in pure cellulose. The cellulose–cellulose interactions include van der Waals forces, hydrogen bonding, dispersion forces, and other forces. For the substituted celluloses, the change in the van der Waals interaction energy after hydrolysis (ΔU_{vdW}) is 103–221% more negative for the substituted celluloses than for pure cellulose as indicated in Table 2. The changes in the electrostatic interaction energy after hydrolysis ($\Delta U_{electrostatic}$) are nearly identical for the substituted celluloses and pure cellulose. After hydrolysis, the substituted celluloses are found to have 1.3–4.4% more hydrogen bonds compared to pure cellulose based on a maximum hydrogen bond length of 3.0 Å. Dispersion forces are thus the main type of interactions that account for the difference in potential energy between the substituted celluloses and pure cellulose after hydrolysis. Since after hydrolysis, substituted cellulose is more stable compared to pure cellulose and before hydrolysis they have similar stability, the hydrolysis reaction occurs more readily for substituted cellulose.

The reason a substituent helps stabilize cellulose after hydrolysis is due to its ability to serve as an anchor to the end of the cellulose chain to which it is grafted. As shown in Fig. 2, the ΔU becomes more negative as the mean square displacement (MSD) of the glucose residual bonded to the substituent decreases, and a regression of the ΔU versus the MSD has an R^2 of 0.87. This indicates that the substituent

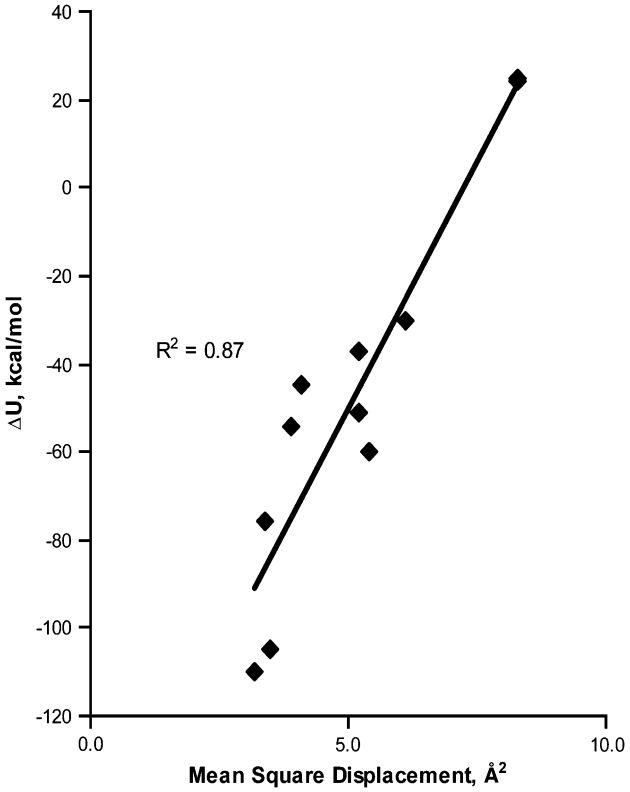

Fig. 2. Change in potential energy for hydrolysis (ΔU) versus the mean square displacement of the glucose residual bonded to the substituent for hydrolyzed pure cellulose, substituted celluloses, and cellulose containing non-bonded C.I. Reactive Blue 19.

reduces the mobility of the glucose residuals near the end of the cellulose chain to which it is grafted, and the term we give for this phenomenon is an anchor effect. The lower mobility of the cleaved substituted cellulose chain therefore allows it to have stronger cellulose–cellulose interactions than are possible in cleaved pure cellulose, especially at 100 °C. A larger substituent serves as a stronger anchor to the cleaved cellulose chain as evidenced by ΔU becoming more negative as the volume of the substituent increases as shown in Fig. 1 and as the MSD of the glucose residual at the end of the cellulose chain decreases as indicated in Fig. 2. Larger substituents therefore increase the ability of the substituent to stabilize cellulose after cleavage, which causes hydrolysis to occur to a greater extent.

Although the potential energies of substituted cellulose and pure cellulose differ 18–79% after hydrolysis, they only differ by 5.1–24% before hydrolysis as shown in Table 2. Substituted cellulose and pure cellulose are more similar in potential energy before hydrolysis because the substituent does not reduce the mobility of the cellulose chain to which it is grafted as much before hydrolysis as it does after hydrolysis since the substituent is positioned far from the end of the cellulose chain before cleavage. In addition, before hydrolysis, the substituted celluloses and pure cellulose have about the same number of hydrogen bonds within 0.2–0.9%, which also explains their similar potential energies. Another reason for the similar potential energy values is that the substituent disrupts some of

the cellulose–cellulose interactions in the system, which increases the potential energy of the system, but the substituent also forms strong interactions with cellulose, which decrease the potential energy. A larger substituent interrupts more cellulose–cellulose interactions and forms more substituent–cellulose interactions as indicated in Table 2 by the increasingly negative values for the potential energy of the substituent–cellulose interactions ($U_{\text{substituent-cellulose}}$) with increasing size of the substituent from mono-substituted acetyl to $C_{18}H_{37}$ quat. This observation explains why a larger substituent has a greater ability compared to smaller substituents to reduce the mobility of the cleaved cellulose chain to which it is bonded and to stabilize cellulose after hydrolysis.

When another molecule is sorbed onto cellulose without being covalently bonded to the polymer, it does not increase hydrolysis of the glycosidic linkages. In the case of Blue 19, non-bonded Blue 19 gives a ΔU value of 24 kcal/mol, which is nearly the same as that of pure cellulose (25 kcal/mol) as shown in Table 2. In addition, non-bonded Blue 19 and pure cellulose have about the same MSD (8.3 Å^2) of the glucose residual at the end of the chain, which indicates that their cleaved cellulose chains have nearly the same mobility. The non-bonded molecule therefore does not increase hydrolysis of the glycosidic linkage because the lack of a covalent bond with cellulose means it cannot reduce the mobility of the cleaved cellulose and therefore does not help stabilize cellulose after cleavage. After hydrolysis, a non-bonded molecule is not necessarily sorbed to a glucose residual at the end of a cellulose chain but is instead sorbed to a different cellulose chain before and after hydrolysis.

3.3. Experimental agreement

Our molecular modeling finding that a substituent on cellulose gives a more negative ΔU than pure cellulose by 55–135 kcal/mol and therefore substantially increases hydrolysis of the glycosidic linkage is supported by experimental data. As hydrolysis approaches equilibrium, the DP of Blue 19-substituted cellulose has been found to be only 31% of the non-substituted cellulose DP, and carboxymethyl cellulose has been reported to have a DP that is only 45% of the DP for non-substituted cellulose [6,9]. In addition, the fact that Blue 19-substituted cellulose has a lower DP than that of carboxymethyl cellulose as hydrolysis approaches equilibrium supports our finding that Blue 19-substituted cellulose has a more negative ΔU of −76 kcal/mol compared to the −37 kcal/mol for carboxymethyl cellulose. Our finding that a substituent on cellulose increases hydrolysis is further supported by studies showing that the sulfite, sulfate, and aldehydo groups also make cellulose more readily hydrolyzed when they are substituted on the polymer [7,8]. The fact that non-bonded Blue 19 gives about the same ΔU as pure cellulose and therefore does not increase hydrolysis is supported by an experiment showing that cellulose with C.I. Direct Red 80 sorbed onto the fiber without being substituted on the cellulose shows about the same extent of hydrolysis of the glycosidic linkages as does non-substituted cellulose [9].

Based on the large difference in ΔU values between the substituted celluloses and pure cellulose, hydrolysis of cellulose predominantly occurs at the glucose residuals bonded to a substituent. This indicates that increasing the degree of substitution results in a greater extent of hydrolysis. Supporting this finding, a past study has reported that increasing the degree of substitution of the carboxymethyl group on cellulose from 0.075 to 0.095 mole/base mole results in a 38% lower cellulose DP as hydrolysis approaches equilibrium [6]. The fact that hydrolysis mainly occurs at the glucose residuals bonded to a substituent also indicates that hydrolysis of the glycosidic linkages approaches equilibrium when no substituent remains on the cellulose fiber.

To find if hydrolysis actually does reach equilibrium when no substituent remains on the cellulose fiber, data were analyzed on the hydrolysis of cellulose grafted to Blue 19 [9]. Eq. 4 was used with the DP and commercial laundering cycle data in Table 1 to obtain the DP as hydrolysis approaches equilibrium (DP_{eq}), and the regression equations shown in Fig. 3 were $(DP - DP_0)^{-1} = -17.5 \times 10^{-3}$ (laundering cycles)$^{-1} - 0.7 \times 10^{-3}$ for Blue 19-substituted cellulose and $(DP - DP_0)^{-1} = -15.9 \times 10^{-3}$ (laundering cycles)$^{-1} - 1.5 \times 10^{-3}$ for pure cellulose. Based on these regressions, Blue 19-substituted cellulose had a DP of 371 at equilibrium while non-substituted cellulose had a DP of 1210. Data for the DP of cellulose bonded to Blue 19 versus the K/S values listed in Table 1 were extrapolated to a K/S of zero. Based on Eq. (5) and the regression equation DP = 214 (K/S) + 330, the DP of Blue 19-substituted cellulose was

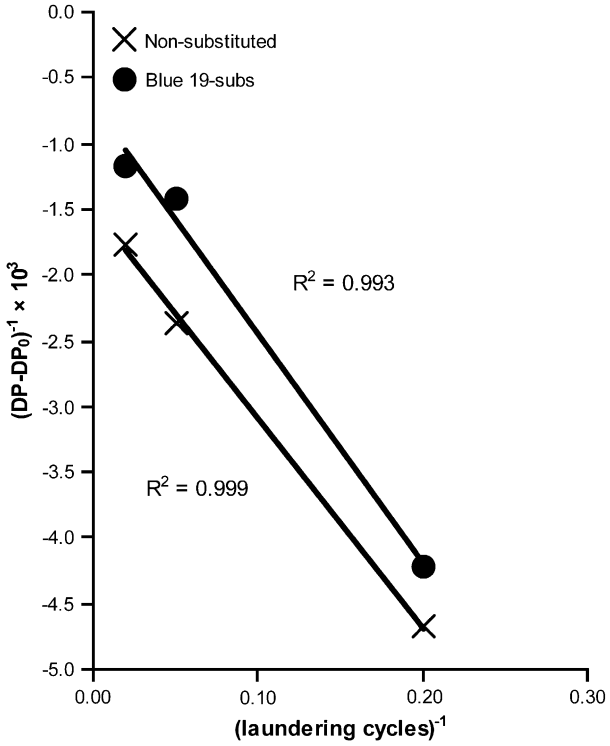

Fig. 3. Linear regression of $(DP - DP_0)^{-1}$ for Blue 19-substituted cellulose and non-substituted cellulose versus (number of laundering cycles)$^{-1}$ with DP_0 being the initial DP. The DP when hydrolysis reaches equilibrium (DP_{eq}) was obtained from the intercept $(DP_{eq} - DP_0)^{-1}$. Blue 19 is C.I. Reactive Blue 19.

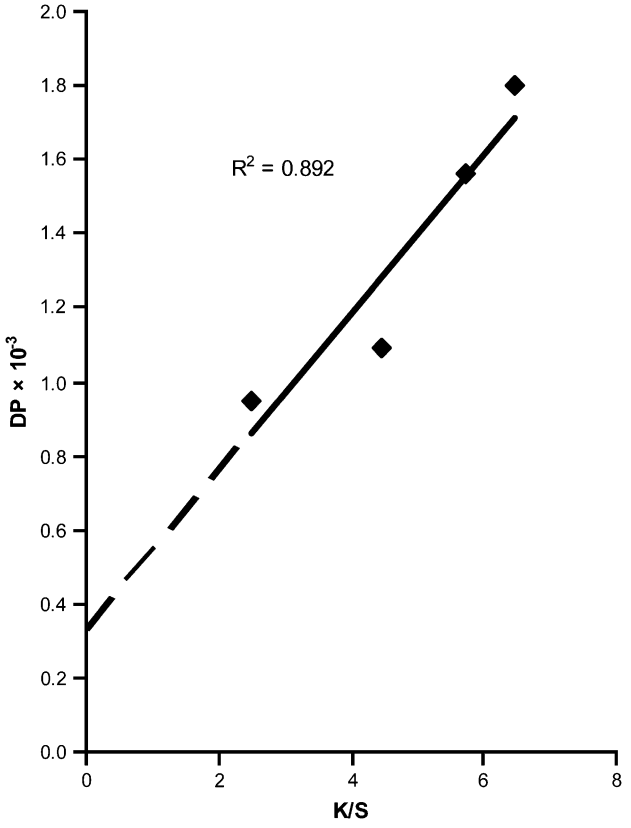

Fig. 4. DP of Blue 19-substituted cellulose at the corresponding K/S value. Regression of the DP versus K/S (solid line) was used to extrapolate (dashed line) the DP to zero concentration of Blue 19 in the cellulose fiber (K/S = 0.0816). Blue 19 is C.I. Reactive Blue 19.

348 when the concentration of Blue 19 in the cellulose fiber was zero as shown in Fig. 4. The DP based on extrapolation to a Blue 19 concentration of zero (348) approximately agrees with the DP based on extrapolation to longer hydrolysis times (371). The experimental data therefore support the finding from molecular modeling that hydrolysis predominantly occurs at the glucose residuals bonded to the substituent and that hydrolysis reaches equilibrium when no substituent remains on the cellulose fiber. The large difference between substituted cellulose and pure cellulose with respect to ΔU values is thus supported by experiment.

4. Conclusion

Molecular modeling has been used to explain how the grafting of various groups onto cellulose increases acid hydrolysis of the β-(1,4)-glycosidic linkages. The substituents included in this study are ester and ether groups of various sizes such as acetyl, carboxymethyl, Blue 19, and various quaternary ammonium compounds. Our molecular modeling indicates that the grafting of these groups onto cellulose increases hydrolysis of the glycosidic linkages by helping to stabilize cellulose after hydrolysis, and larger substituents increase hydrolysis to a greater extent. After hydrolysis of substituted cellulose, the substituent is positioned at the end of the cleaved cellulose chain to which it is bonded. The substituent serves as an anchor to the cleaved cellulose chain by reducing the mobility of the cleaved cellulose, which allows it to have stronger cellulose–cellulose interactions compared to cleaved pure cellulose, especially at 100 °C. The substituent serves as an anchor to the cleaved cellulose chain to which it is bonded because it forms strong interactions with the cellulose chains. As the size of the substituent increases, the cellulose–substituent interactions become stronger, which increases the ability of the substituent to reduce the mobility of the cleaved cellulose. As a result, the ability of the substituent to stabilize cellulose after hydrolysis increases with the size of the substituent. Substituted cellulose and pure cellulose are more similar in potential energy before hydrolysis because the substituent interrupts some of the cellulose–cellulose interactions in the system and also forms strong interactions with cellulose. The molecule must be substituted on cellulose to increase hydrolysis because in the case of Blue 19 sorbed onto cellulose without being covalently bonded to the polymer, Blue 19 does not reduce the mobility of the cleaved cellulose, and it thus does not allow for stronger cellulose–cellulose interactions compared to pure cellulose. Since the cause for increased hydrolysis of the glycosidic linkages is the substituent helping to stabilize cellulose after hydrolysis, perhaps all types of substituents on cellulose increase hydrolysis of the glycosidic linkage. Van der Waals forces are the main type of intermolecular interaction that contributes to the greater stability of substituted cellulose compared to pure cellulose after hydrolysis.

Supporting our finding that the grafting of various groups onto cellulose substantially increases hydrolysis of the glycosidic linkages, experiments have shown that as hydrolysis approaches equilibrium, the DP of carboxymethyl cellulose and cellulose bonded to Blue 19 are only 45% and 31%, respectively, of the DP for non-substituted cellulose. In addition, the lower DP of the Blue 19-substituted cellulose compared to carboxymethyl cellulose as hydrolysis approaches equilibrium supports our finding that Blue 19 gives a more negative ΔU than the carboxymethyl group. Based on the large difference between substituted cellulose (−110 to −30 kcal/mol) and pure cellulose (25 kcal/mol) with respect to the change in potential energy for hydrolysis (ΔU), hydrolysis of the glycosidic linkages mainly occurs at the glucose residuals bonded to the substituent. This indicates that the extent of hydrolysis increases with increasing degree of substitution. Experiments have confirmed this finding as increasing the degree of substitution of the carboxymethyl group on cellulose has led to a lower cellulose DP after hydrolysis. Our finding that hydrolysis mainly occurs at the glucose residuals bonded to the substituent is also supported by experiments showing that hydrolysis of cellulose approaches equilibrium when no substituent remains on the cellulose fiber. The supporting experiments therefore prove that molecular modeling can be used to study this phenomenon.

Acknowledgements

This work was completed utilizing the Research Computing Facility of the University of Nebraska – Lincoln.

Financial supports from the University of Nebraska – Lincoln Agricultural Research Division, and funds through the Hatch Act are gratefully acknowledged. The authors also acknowledge Dr. Joan Laughlin for the support to David Karst through the Laughlin Fellowship.

References

[1] Reddy N, Yang Y. AATCC Rev 2005;5:24–7.
[2] Reddy N, Yang Y. Polymer 2005;46:5494–500.
[3] Reddy N, Yang Y. Green Chem 2005;7:190–5.
[4] Reddy N, Yang Y. Trends Biotechnol 2005;23:22–7.
[5] Alen R, Sjostrom E. Degradation conversion of cellulose-containing materials into useful products. In: Nevell TP, Zeronion S, editors. Cellulose chemistry and its applications. New York: John Wiley & Sons; 1985. p. 531–44.
[6] Borsa J, Tanczos I, Rusznak I. Colloid Polym Sci 1990;268(7):649–57.
[7] Luetzow AE, Theander O. Svensk Papperstidning 1974;77(9):312–8.
[8] Ranby BG, Marchessault RH. J Polym Sci 1959;36:561–4.
[9] Yang Y, Hughes JE. Textile Chem Color 1997;29(11):23–9.
[10] Nevell TP. Degradation of cellulose by acids, alkalis, and mechanical means. In: Nevell TP, Zeronion S, editors. Cellulose chemistry and its applications. New York: John Wiley & Sons; 1985. p. 223–42.
[11] Accelrys Inc. MS Modeling 3.0. San Diego: Accelrys; 2003.
[12] Karst D, Yang Y. Polymer 2006;47:4845–50.
[13] Mauersberger HR. Matthews' textile fibers. 5th ed. New York: John Wiley & Sons; 1947.
[14] Ott E. Cellulose and cellulose derivatives. New York: Interscience Publishers; 1946. p. 214.
[15] Young RA. Structure, swelling and bonding of cellulose fibers. In: Young RA, Rowell RM, editors. Cellulose structure, modification and hydrolysis. New York: John Wiley & Sons; 1986. p. 91–128.
[16] Cramer CJ. Essentials of computational chemistry: theories and models. New York: John Wiley & Sons; 2002. p. 46, 82–4.
[17] Louise-May S, Auffinger P, Westhof E. Curr Opin Struct Biol 1996;6(3):289–98.
[18] Sun HJ. Comput Chem 1994;15(7):752–68.
[19] Sun H, Mumby SJ, Maple JR, Hagler AT. J Am Chem Soc 1994; 116(7):2978–87.
[20] Sun H. Macromolecules 1995;28(3):701–12.
[21] Feughelman M. The mechanical properties of fibres and fibre thermodynamics. In: Happey F, editor. Applied fibre science, vol. 1. New York: Academic Press; 1978. p. 43–68.
[22] Hughes JH. An investigation of the mechanisms causing tendering of 100% cotton fabrics after repeated commercial launderings. Master's thesis, Institute of Textile Technology, Charlottesville; 1996.
[23] Fan LT, Gharpuray MM, Lee Y. Acid hydrolysis of cellulose. In: Fan LT, Gharpuray MM, Lee YH, editors. Biotechnology monographs: cellulose hydrolysis, vol. 3. New York: Springer-Verlag; 1987. p. 121–48.
[24] Fujino K, Fujimoto F. Sen'I Gakkaishi 1961;17:178–80.